Published in final edited form as:
J Comp Neurol. 2013 May 1; 521(7): 1497–1509. doi:10.1002/cne.23237.

Properties of the ON Bistratified Ganglion Cell in the Rabbit Retina

Hideo Hoshi[1,2], **Lian-Ming Tian**[1], **Stephen C. Massey**[1], and **Stephen L. Mills**[1]

[1]Department of Ophthalmology and Visual Science, University of Texas at Houston, 6431 Fannin, MSB 7.024, Houston, Texas 77030

[2]Department of Psychology, Graduate School of Humanities and Sociology, The University of Tokyo, Bunkyo-ku, Tokyo 113-0033, Japan

Abstract

The identity of the types of different neurons in mammalian retinae is now close to being completely known for a few mammalian species; comparison reveals strong homologies for many neurons across the order. Still, there remain some cell types rarely encountered and inadequately described, despite not being rare in relative frequency. Here we describe in detail an additional ganglion cell type in rabbit that is bistratified with dendrites in both sublaminae, yet spikes only at light onset and has no response bias to the direction of moving bars.

This ON bistratified ganglion cell type is most easily distinguished by the unusual behavior of its dendritic arbors. While dendrites that arborize in sublamina *b* terminate at that level, those that ascend to arborize in sublamina *a* do not normally terminate there. Instead, when they reach the approximate radius of the dendrites in sublamina *b*, they dive sharply back down to ramify in sublamina *b*. Here they continue to course even further away from the soma at the same level as the branches wholly contained in sublamina *b*, thereby forming an annulus of secondary ON dendrites in sublamina *b*. This pattern of branching creates a bistratified dendritic field of approximately equal area in the two sublaminae initially, to which is then added an external annulus of dendrites only in sublamina *b* whose origin is entirely from processes descending from sublamina *a*. It is coupled to a population of wide-field amacrine cells upon which the dendrites of the ganglion cell often terminate.

Keywords

ganglion cell; bipolar cell; amacrine cell; uniformity detector

The ganglion cells of the retina form numerous parallel visual channels which deliver substantially different transforms of visual information to the various central targets they innervate (Roska and Werblin, 2001; Wässle, 2004). While there is some variation among ganglion cell types across mammalian species, there are many similarities, including the most-characterized of the at least 15 types in the rabbit retina (Marc and Jones, 2002; Rockhill et al., 2002; Roska and Werblin, 2001). These numerous ganglion cell types follow

Corresponding author: Stephen L. Mills, Stephen.L.Mills@uth.tmc.edu, Phone: (713)500-5998, Fax: (713)500-0682.

Conflict of Interest: The authors have no conflicts of interest.

Role of authors: All authors had full access to all the data in the study and take responsibility for the integrity of the data and the accuracy of the data analysis. Study concept and design: all. Acquisition of data: HH, MLT. Analysis and interpretation of data: all. Drafting of the manuscript: SLM. Critical revision of the manuscript for important intellectual content: all. Statistical analysis: SLM. Obtained funding: SLM, SCM. Administrative, technical, and material support: all. Study supervision: SLM.

the stratification rules of the retina in general, in that those which ramify in sublamina *a* spike at light offset, those that ramify in sublamina *b* spike at light onset, and those that are bistratified may spike transiently both at light onset and offset. The only fully bistratified ganglion cell in the Rockhill et al. (2002) catalog was the ON-OFF directionally selective ganglion cell (G7), but recently, other types of bistratified ganglion cell have been described, including a transient ON-OFF ganglion cell (Sivyer et al., 2011), a uniformity detector (Sivyer et al., 2010; Sivyer and Vaney, 2010), and an ON bistratified ganglion cell (Hoshi et al., 2009; Roska et al., 2006). Additionally, one type of intrinsically photosensitive retinal ganglion cell (ipRGC) is bistratified in retinas of mouse, monkey, and rabbit (Hattar et al., 2002; Viney et al., 2007; Liu et al., 2008).

Here we describe for the first time the detailed morphological and population properties of an ON bistratified ganglion cell type in rabbit that stratifies in both sublaminae, yet spikes only at light onset and has no response preference to the direction of moving bars, firmly distinguishing it from the ON-OFF DS ganglion cell. We have previously shown that this ganglion cell contains spines on its dendrites in sublamina *a* which contact ON bipolar cells as their axons descend through the OFF sublamina (Hoshi et al., 2009). Synaptic ribbons and glutamate receptors are also present at these conjunctions. We suggest this cell, which we previously called the bistratified diving ganglion cell, is the same as the ON bistratified cell (Roska et al., 2006; Roska and Werblin, 2001), but clearly distinct from the other bistratified types.

Materials and Methods

Adult rabbits were deeply anesthetized with injections of urethane (1.5 g/kg i.p.), then humanely killed by intracardial injection of 5 cc urethane following removal of the eyes. All procedures were in accordance with the guidelines of the University of Texas at Houston Animal Welfare Committee. Early morphological classifications were derived solely using albino rabbits; later combined morphological/physiological characterization was made using either albino or pigmented rabbits. Some retinas were removed from the sclera and placed on a black membrane filter, ganglion cell side up, inserted into a perfusion chamber (Warner Instruments, Hamden, CT) and then placed on the stage of an Olympus BX50WI upright epifluorescent microscope. Other retinas were cut into pieces and placed into the perfusion chamber with the sclera attached. The tissue was superfused during the experiment with Ames medium (Sigma-Aldrich Inc., St. Louis, MO) bubbled with 95% O_2/5% CO_2.

Cell targeting, electrophysiology, and injection

Ganglion cells were stained by application of a few drops of the fluorescent stain acridine orange (0.0001%; Invitrogen, Carlsbad, CA) dissolved in Ames medium and applied to the retina as needed to visualize the ganglion cell population, or following diffusion of PoPro1 (Invitrogen) from a 1 mM injection into the optic nerve 12 hr prior to isolation of the retina. Ganglion cells were visualized through the epifluorescent microscope with a 40x water objective and a blue-violet excitation filter (400–440 nm). With experience, several ganglion cell types can be targeted with high efficiency, including the ON bistratified ganglion cell described in this study. When labeled with either fluorescent dye, the ON bistratified ganglion cell can be distinguished as having a dimly labeled, medium small soma with little discriminable nucleus. It appears “bottle shaped”, being elongated with a small portion of the primary dendrite forming a visible “neck” at one end. Cells meeting this description were revealed to be ON bistratified ganglion cells > 90% of the time.

Ganglion cells targeted with acridine orange or Popro1 were stained via iontophoresis of Neurobiotin. Thinwall glass microelectrodes pulled with a Brown-Flaming horizontal micropipette puller (Sutter Instruments, P-97) were tip-filled with 1% Lucifer Yellow-CH

(L-453, Invitrogen) and 3.5% Neurobiotin (Vector Labs, Burlingame, CA) in 50 mM phosphate buffer and backfilled with 3M LiCl. In early experiments aimed at morphological characterization, Lucifer Yellow was iontophoresed with 1 nA negative current for a few seconds to verify cell penetration and obtain a preliminary identification of the cell type, then each ganglion cell was filled with Neurobiotin (+1 nA, 3 Hz, 10 min). For later experiments that included recording, loose patch recordings were made with 1.2 mm borosilicate glass pulled to a resistance of 4–6 MΩ and filled with Ames medium and 0.2% pyranine (Sigma-Aldrich). Recordings were made with an NPI EPC-03X amplifier (ALA Scientific, Westbury, NY) at 1000X gain and notch filtered at 60 Hz. Data was acquired and analyzed using data acquisition sytems from Experimenter 5.0 (DataWave Technology, Berthoud, CO) or Spike 2/Power 1401 (CED Limited, Cambridge England). Following physiological characterization, the recorded cells were filled either with a sharp electrode, as described above, or by electroporation with the recording electrode following the protocol of Kanjhan and Vaney (2008). Ligands for the mGluR6 and GABA receptors, L-APB (L-2-amino-4- phosphonobutyrate), LY341495 and SR95531, were obtained from Tocris, Inc. and added to the perfusate.

Immunohistochemistry and antibody characterization

Tissue was fixed in 4% paraformaldehyde in 0.1M phosphate buffered saline (PBS), pH 7.4, for 1 hour at room temperature. Cells were visualized by overnight incubation in 1:1000 streptavidin-Cy3 (Jackson ImmunoResearch, West Grove, PA). Tissue was mounted in 50% 0.2M PBS + 50% glycerol +0.1% para-phenylenediamine (Sigma) to retard fading by fluorescent illumination. For triple-labeling, some retinas were blocked with 3% donkey serum (Jackson)/0.1% sodium azide/0.1M PBS for 90 min at room temperature and incubated in primary antibodies with 0.1M PBS/0.1% sodium azide/0.3%TritonX-100 for 7 days at 4°C. Then, tissues were rinsed several times in 0.1 M PBS and reincubated in the secondary antibody overnight at 4°C. Donkey anti-mouse Cy3, donkey anti-goat Cy5 (Jackson, 1:200) and donkey anti-rabbit Alexa488 (Invitrogen, 1:200) were used as secondary antibodies.

An antibody to choline acetyltransferase (ChAT; 1:100; Millipore; immunogen = human placental enzyme) was used as a reference marker in establishing the depth of stratification, The specificity of the ChAT antibody was tested previously by Western blot analysis of brain protein extracts from rat and a variety of fish (Anadón et al., 2000) and showed bands of 68–72 kDa. All bands disappeared when the primary antibody was preincubated with human placental ChAT.

The RIBEYE antibody was generated against recombinant mouse CtBP2 and recognizes synaptic ribbons in mammalian retinas (Schmitz et al., 2000; tom Dieck et al., 2005). Western blots using protein lysates from wildtype E10.5 mouse embryos showed staining of the appropriate 48kDa band. There was no staining in similar blots using tissue from mice with mutations that eliminate expression of CtBP2 (Hildebrand and Soriano, 2002). Calbindin-28 kDa was reported by the manufacturer to stain the appropriate 27–28 kDa band in immunoblots from brain tissue of rat, chicken, monkey and mouse, and was demonstrated by Massey and Mills (1996) to label a specific type of ON cone bipolar cell in rabbit retina. The TOH antibody was demonstrated to show selective immunoblotting by the manufacturer using an extract of cultured rat adrenal pheochromocytoma (PC12) cells and is well characterized as a marker for dopaminergic amacrine or interplexiform cells in the retina. Also, aliquots of solubilized human adrenal medullas and solublized 3T3 cells expressing human TOH, but not non-cognate forms of recombinant human TOH stained appropriate 60–66 KDa bands in Western blots (Lewis et al. 1993).

The GABA antibody (Immunosolution, Inc., Jesmond, NSW, AU; 1:1,000) was raised as a formaldehyde conjugate to the carrier protein porcine thyroglobulin and used to test for the transmitter identity of the coupled amacrine cells. The antibody was reported by the manufacturer to recognize GABA, but not formaldehyde-conjugates of other amino acids transmitters in dot blots, nor glutaraldehyde conjugates of GABA (Pow et al., 1995). It also recognized previously established GABA-containing, but not glycine-containing, neurons in a variety of tissues. As a final control, we cut vibratome sections of rabbit retina at 50 μm thickness on a Leica VT1000S vibratome (Leica Microsystems, Bannockburn, IL). We then preadsorbed porcine thyroglobulin (Sigma-Aldrich) for 1 hr in 10X or 1000X molar excess over the antibody concentration (1:1000). The sections were incubated in antibody overnight, then rinsed and visualized with a Cy3-conjugated secondary. The pattern and intensity of anti-GABA immunostaining in sections preadsorbed with thyroglobulin was indistinguishable from untreated sections, indicating that possible clones recognizing the carrier protein did not contribute false positives to the analysis.

Confocal microscopy

Fluorescent images of stained material were acquired using a Zeiss LSM 510 Meta confocal microscope. The size and number of the optical sections obtained are specified in each figure. Intensity adjustments were made in Adobe Photoshop (Adobe Systems, Inc.) to optimize dynamic range and contrast. In some cases, the Zeiss software LSM Image Browser was used to code stratification depth as a function of color.

Visual stimulation

Each ganglion cell was stimulated with spots, annuli, and moving bars imaged on a Lucivid monitor (Microbrightfield, Inc, Williston, VT) and projected through a 4X or 10X objective onto the retina using custom routines written in MatLab (The Mathworks, Natick, MA) and the Psychophysics Toolbox (Brainard, 1997; Pelli, 1997). Pieces of retina were always placed with the visual streak oriented in the same direction so that directional preferences could be reliably recovered. Receptive field sizes were mapped by flashing spots of light ranging from 30–900 μm in diameter. Light spots were at 100% contrast. Reversal of the foreground and background brightnesses adapted the cell to a large degree, so dark spots were flashed at 50% contrast against a gray background.

Calculations of directional selectivity

Differential sensitivity to direction of motion was determined by moving a 50 μm width bar across the receptive field at orientation intervals of 45° at a speed of 200 μm sec^{-1}. Faster speeds were examined without evidence of increased directional preference. An index of directional selectivity (DSI) was calculated by the formula:

$$\mathrm{DSI}=\sum_{d}\frac{\overrightarrow{N_d}}{R_d}$$

where N_d are the vectors for each of the 8 directions and R_d is the sum of the magnitudes for the 8 directions (Taylor and Vaney, 2002; Farrow and Masland, 2011). The DSI can vary from 0 to 1, where the firing rate is equal for all directions (0) or restricted to a single direction (1). For each cell, the sequence of bar stimuli was repeated to give an assessment of variability across directions vs. that within a direction. The spiking rates for each direction of a trial of 8 was normalized by the overall spiking to remove variation between cells and between trials, giving the best opportunity to reveal directional preferences. To assess relative significance of the results, a Monte Carlo simulation was performed in

MatLab whereby the DSI for 1,000,000 trials was calculated by drawing the spiking rates for the 8 directions randomly from a pool of pseudorandom numbers with the same mean and distribution as the normalized spike rates of the actual data.

Results

Morphology of the ON bistratified ganglion cell

ON bistratified ganglion cells can be distinguished by a combination of size, stratification depth, branching pattern, morphology and physiology from the other bistratified ganglion cells in the rabbit retina, such as the partly bistratified G3 ganglion cell (Hoshi and Mills, 2009) and the ON-OFF directionally selective ganglion cell (Amthor et al., 1984; Famiglietti, 1983). We previously have called this new type of bistratified ganglion cell the bistratified diving ganglion cell because of its most diagnostic feature (Hoshi et al., 2009), namely that some of the dendrites that branch in sublamina *a* do not terminate there, but descend back to stratum 4/5 as they approach the edges of the dendritic field. They terminate there at the same depth as the ON arbor of the cell, but more distant from the soma than the ON dendrites that remain exclusively in sublamina *b*. Figure 1 illustrates this by color-coding the component dendritic arbors. Fig. 1A and Fig. 1B show the dendritic arbors in sublamina *a* and *b*, respectively. Notice that there are several “orphan” dendrites in Fig. 1B that do not appear connected to the rest of the arbor. With a high magnification objective, this is a diagnostic feature of these cells. In Fig. 1C, the orphan dendrites are colored green to highlight the separation from the terminations of the rest of the ON dendrites. Fig. 1D demonstrates that these orphan dendrites in sublamina *b* arise from the OFF arbor, as seen by comparison of Figs. 1B and 1D. This demonstrates that the dendrites that ramify in sublamina *b* which initially appear isolated can be traced back to the somas by following them first up to the arbor in sublamina *a* and then back to the soma.

Fig. 2 shows in more detail the diving pattern of these cells. Fig. 2A is an example of an ON bistratified ganglion cell depth coded by color. Blue denotes the depth of the arbor at the most extreme extent of dendrites in sublamina *a*. Colors shift toward the red with increasing depth as focus is moved toward the ganglion cell layer and the most proximal dendrites in sublamina *b* appear red. Green portions of processes are represented by: (1) processes in sublamina *b* that are ascending to sublamina *a*, (2) processes in sublamina *a* that are descending back to sublamina *b*, and occasionally, (3) processes emanating close to the soma in sublamina *b* that ascend briefly more distal to the level of the *b* arbor before descending to the *b* level and arborizing more fully. Only the second type are representative of the characteristic pattern of an annular diving region seen in Figs. 2A,B.

The “orphaned” annular dendrites of 10 ON bistratified ganglion cells that were not affected by overlapping processes from neighboring ganglion cells or coupled amacrine cells or by local irregularities in depth were selected for analysis. Fig. 2B is a composite of these annular processes color coded for depth of dendrites. Adobe Photoshop was used to adjust all cells to the same diameter, then the diving dendrites were clipped from each micrograph and superimposed on a common template. Some slight radial shifting was done to minimize overlap between processes from different cells, but each set remained at its true distance from the soma. This figure emphasizes that almost all of the recurrent dendrites originate at the terminations of the dendrites in sublamina *a* and descend to sublamina *b* in the annular region.

The average number of terminal diving processes for the 10 cells in Fig. 2B was 7.2 (standard deviation (s.d) = 3.33) diving processes per cell. It can be seen that, with a single exception, dendrites did not begin to dive until they approached the peripheral region of the cell. It can also be seen that all processes dive from the OFF sublamina toward the ON

sublamina. This distinguishes them morphologically from recent descriptions of uniformity detectors in rabbit (Sivyer et al., 2010; Sivyer and Vaney, 2010), which are also bistratified at similar depths. The dendrites of these cells change depths irregularly throughout the dendritic field and also have an abbreviated tertiary ramification in the middle of the inner plexiform layer.

Relative sizes of the dendritic arbors and density of the ON bistratified ganglion cell

We began by staining and morphologically characterizing 76 ON bistratified ganglion cells across the retina; 31 retinas from albino rabbits were represented in this sample. No physiology was obtained at this time. As noted, dendrites that ramified exclusively in sublamina *b* formed an ON arbor which was about the same size as the OFF arbor in sublamina *a*. Due to the annular extension of the ON arbor formed by the diving dendrites, the total ON arborization was consistently larger than the OFF arbor (Fig. 3A). Equivalent dendritic diameters were calculated by measuring the circumscribed area of each dendritic arbor, then calculating the equivalent diameter for each of those areas. The equivalent diameter of the OFF arbor varied in size from about 200 μm near the visual streak to about 630 μm in the periphery, while the equivalent diameter of the total ON arbor increased from about 280 μm to about 640 μm over the same range. The ratio of the diameters of the total ON to OFF arbor was 1.4, s.d. = 0.17, (Fig. 3B) and did not vary across the retina in a consistent manner.

Some of the injected ON bistratified ganglion cells showed Neurobiotin-staining to their neighboring ganglion cells. These did not occur regularly enough to obtain reliable density counts across the retina. Nevertheless, the mean distance between the injected ganglion cells and their coupled neighbors can provide an estimate of the coverage factor at these locations. The average distance was calculated for all nearest neighbor distances for 7 of these injected cells and normalized by the dendritic radius. The mean distance was 1.1 radii (s.d. = 0.24). The coverage factor is calculated as the product of density and area. We estimated the density as the inverse of squared mean cell spacing, where: mean cell spacing^2 = the center-to-center spacing^2 multiplied by (√3)/2 for hexagonal arrays (Lamb and Simon 1976). These calculations predict a coverage factor of 3.1 for ON bistratified ganglion cells. If a coverage factor of 3.1 were consistent across the retina, this would predict densities from about 10–20 cells/mm^2 in the midperiphery, where most of our cells were sampled. Density measurements taken from intercellular distances of a few instances of coupled ganglion cells produce more variable measurements than samples from larger populations, so the density measurement should be interepreted with caution.

Together, these measurements indicate that the ON bistratified ganglion cell is not a rare ganglion cell, despite the paucity of prior descriptions of it in the literature. It is intermediate in density among rabbit ganglion cells, which range from about 550–850 cells/mm^2 for G1 ganglion cells (local edge detectors) in the visual streak (van Wyk et al. (2006) to 2 cells/mm^2 for α ganglion cells, as estimated by Rockhill et al., (2002), who used an average coverage factor of 1.8 to calculate densities of ganglion cells whose size but not densities were known.

Comparison of the ON bistratified ganglion cell with other bistratified ganglion cells

Fig. 4A shows a ON bistratified ganglion cell (left) adjacent to an ON-OFF DS ganglion cell (right), the most well-characterized bistratified ganglion cell in the rabbit retina. Although we did not make systematic measurements of ON-OFF DS ganglion cells across the retina, we found that ON bistratified ganglion cells were always larger than ON-OFF DS ganglion cells that were stained in the near vicinity. In addition to the substantial size difference, ON bistratified ganglion cells were always coupled to amacrine cells, as will be described, while

ON-OFF DS ganglion cells were usually uncoupled, except for a small percentage that were coupled almost exclusively to neighboring ON-OFF DS ganglion cells (Vaney, 1994). Homologous Neurobiotin-coupling from the injected ON bistratified ganglion cell to its neighbors can be seen in Fig. 4A (arrows); whether these were stained via direct gap junctional coupling or indirectly via amacrine cells was indeterminate.

Other distinctive differences between ON bistratified ganglion cells and ON-OFF DS ganglion cells lay in the branching pattern and the level of stratification. ON-OFF DS ganglion cells are well known to branch frequently at right angles, thereby forming characteristic loops (Famiglietti, 1983; Vaney, 1994). Further, while the dendrites of ON-OFF DS ganglion cells lie within the two strata formed by the processes of starburst amacrine cells (Fig. 4C), the dendrites of ON bistratified ganglion cells lie just outside these bands (Fig. 4B). Specifically, the outer dendrites in sublamina *a* lie distal to the starburst amacrine cell band in sublamina *a*, shown stained with an antibody to choline acetyltransferase (ChAT). The inner dendrites in sublamina *b* lie proximal to the starburst amacrine cell band in sublamina *b*. The distance from the soma at which the diving processes leave sublamina *a* and dive to sublamina *b* is typically where the dendrites that arborize exclusively in sublamina *b* terminate (Figs. 4D, 2B).

Figure 4E shows a z-reconstruction of a uniformity detector (Amthor et al., 1989; Sivyer et al., 2010; Sivyer and Vaney, 2010), which illustrates some of the differences in stratification between this type of cell and ON bistratified ganglion cells. The most obvious difference is the inclusion of additional branches in the middle of the inner plexiform layer in the uniformity detector, consistent with previous reports (Sivyer and Vaney, 2010; Sivyer et al., 2010). Another reliable difference was the manner in which processes changed their level of stratification, which was consistently annular for ON bistratified ganglion cells. This contrasts with a less regular change throughout the dendritic field for 5 uniformity detectors we sampled in the area from 5–10 mm inferior to the visual streak) and those illustrated by Sivyer and Vaney (2010). The identity of each of the uniformity detectors we stained was confirmed by physiology consistent with that reported by Sivyer et al. (2010), namely, continuous spiking except at the onset of light or dark stimuli and the presence of complex spikes.

Tracer coupling in ON bistratified ganglion cells

Injection of Neurobiotin into individual ON bistratified ganglion cells invariably stained a population of wide-field amacrine cells. Fig. 5A is color coded for depth and shows that the somas of these cells are displaced to the ganglion cell layer (Fig. 5A, magenta). Double-labeling with an antibody to GABA demonstrated that these wide-field amacrine cells contained GABA (Fig. 5B–D). The coupled amacrine cells have a moderately large, nearly circular soma from which 2 dendrites emerge in a bipolar fashion (Fig. 5A, 6A). Further branching typically begins at about 10 μm or more from the soma. An interesting regularly recurring feature is that a dendrite of the ganglion cell terminates upon a dendrite of a coupled amacrine cell (Fig. 6B–D), rather than contacting it *en passant* as is more commonly seen in other ganglion/amacrine coupled pairs. These polyaxonal wide-field amacrine cells make tip-to-branch contact with the diving cell dendrites and dendro-dendritic contacts with other tracer coupled amacrine cells at both stratum 1 and stratum 5. Additionally, the coupled amacrine cell dendrites often contact the ganglion cell dendrites at spines and varicosities, which are generally found to be sites of synaptic input.

Among the tracer-couple amacrine cells, we sometimes found a smaller medium-sized amacrine cell which also ramified in stratum 4, but whose somas were conventionally placed in the inner nuclear layer (Fig. 5A; smaller green somas; arrows).

Possible synaptic connections made by ON bistratified ganglion cells

Hoshi et al. (2009) showed that the dendrites of the ON bistratified ganglion cell received inputs from a bipolar cell that can be labeled with antibodies to calbindin-28K Da (Massey and Mills, 1996). In sublamina *a*, these synaptic contacts were made ectopically by ribbons in the descending axons in stratum 1 of the inner plexiform layer, while contacts in sublamina *b* were made by conventional ribbons in the axon terminals of the calbindin-positive bipolar cell; this was true both for the recurrent arbor of the ON bistratified ganglion cell as well as the arbor confined exclusively to sublamina *b*. Fig. 7A, B (arrows) show how the processes of a Neurobiotin-stained ON bistratified ganglion cell (green) send out spines that contact the axon terminals of the calbindin-positive bipolar cell (blue) while Fig. 7C demonstrates that these ganglion cell processes (magenta) appose ribbon synapses (green).

Physiology of ON bistratified ganglion cells

ON bistratified ganglion cells responded to onset of light or offset of dark spots (1 sec onset/1 sec offset) with a train of spikes (Fig. 8A) at a latency in the range of 65–100 ms (mean = 78 ms; s.d. = 10 ms). Increasing the diameter of the light spot produced more transient responses together with an increase in spiking at light offset and produced a size-response curve peaking near the dendritic field diameter (Fig. 8B). Dark spots decreased spiking with increased spot size (Fig. 8C). L-APB (25 μM) abolished light-driven spiking (Fig. 8B,C). These were the primary physiological characteristics that suggested that the recorded cell was of the ON bistratified type; only those confirmed by morphology were included in the analysis.

We also investigated the possibility that an excitatory OFF bipolar input was masked by hyperpolarization of ON circuits by L-APB. This was done by adding the mGluR6 antagonist LY341495 (50–100 μM) to L-APB or occasionally alone. LY341495 presumably repolarized the ganglion cells, as spiking was restored. This could potentially reveal OFF bipolar cell activity normally masked by the dominant ON bipolar cell input, but the results indicated that the restored spiking activity was not light-driven (Fig. 8B,C). LY341495 alone also produced sustained spiking that was not stimulus-driven (not shown.) These results support prior data that excitatory input to ON bistratified cells arises only from ON bipolar cell input (Roska and Werblin, 2003), either in sublamina *b* or from ectopic axonal ribbons from ON bipolar cells in sublamina *a* (Hoshi et al. (2009).

Directional selectivity

ON-OFF DS ganglion cells are directionally-selective over a broad range of velocities, while ON-DS ganglion cells are selective only to slow velocities (Oyster, 1968; Wyatt and Daw 1975). The response of ON bistratified ganglion cells to moving bars of light was assessed using bars of 40 μm width and a velocity of 100 μm/s. Velocities of 200, 400 and/or 800 μm/s were often investigated, but were no more directional than the slow speed and are not illustrated here. Directional selectivity was assessed by calculating the DSI, as described.

Fig. 8D shows representative responses and a polar plot for a single ON bistratified ganglion cell located 5.7 mm inferior to the visual streak, while Fig. 8E, F shows the aggregate results for 18 cells. The average DSI for these cells was 0.061 (Fig. 8E), compared to DSIs in the range of 0.24 to 0.9 for ON-OFF DS ganglion cells and transient or sustained ON DS ganglion cells in both rabbit and mouse (Taylor and Vaney, 2002; Farrow and Masland, 2011). Simulations with random spiking rates with the same mean and distribution as the actual data produced a mean of 0.051 and a standard deviation of 0.026. This difference was not significant from the actual data ($z = 0.38$, $p > 0.05$), suggesting no significant directional organization exists in the real data. Other features of the data also suggested a lack of

directional preference. Known DS cells have directional preferences that cluster in 3 or 4 cardinal directions (Oyster and Barlow, 1967; Kanjhan and Sivyer, 2010; Hoshi et al., 2011), but the distribution of the vector directions for ON bistratified ganglion cells showed no clear clusters with respect to direction (Fig. 8F).

Finally, directional-selectivity is abolished in all types of DS ganglion cells in the rabbit retina in response to the application of $GABA_a$ antagonists (Caldwell et al. 1978). Addition of 25 μM SR95531 to the perfusate did not decrease the DSI index in 4 ON bistratified ganglion cells tested under control and drug conditions (not shown). Indeed, 3 of the 4 cells tested had nonsignificant increases in DSI in the presence of SR95531.

Discussion

The ON bistratified ganglion cell has a distinctive morphology diagnostic for this class of ganglion cell. In particular, the diving behavior of the dendrites that ascend to sublamina *a*, but terminate in an annular pattern in sublamina *b*, creates a branching pattern in this cell that is unique. It is also unusual for a ganglion cell to ramify extensively in one of the sublamina without receiving excitatory input from the bipolar cells in that sublamina. An exception is the uniformity detector, which is reported to lack excitatory input in either layer (Sivyer et al. 2010). However, the physiology we have shown is inconsistent with that of the uniformity detector as shown by Amthor et al., (1989), Sivyer et al. (2010) and our own recordings from uniformity detectors.

Famiglietti proposed that there are three types of bistratified ganglion cell in the rabbit retina based on Golgi material (Famiglietti, 2009). His BS1 corresponds to the well known ON-OFF directionally selective ganglion cell. His material contained additional stained bistratified ganglion cells, from which he further proposed two new bistratified classes, BS2 and BS3. Both BS2 and BS3 initially stratified similarly to our ON bistratified ganglion cell; one of his examples appears to contain a process that dives from sublamina *a* to sublamina *b* in the periphery of its dendritic field.

The ON bistratified ganglion cell can be distinguished from all other known bistratified ganglion cells previously described in the rabbit retina. These include the ON-OFF directionally selective ganglion cell (Barlow et al., 1964; Taylor and Vaney, 2002), an intrinsically photosensitive retinal ganglion cells (ipRGC) containing melanopsin, which occur in multiple morphological types, including one which is bistratified (Hattar et al., 2002; Viney et al., 2007). The extremely sparse morphology of ipRGCs does not resemble that of ON bistratified ganglion cells, nor is the coupling pattern seen following Neurobiotin injection into an ipRGC similar to that of ON bistratified ganglion cells. The ON bistratified ganglion cell is not directionally-selective, further distinguishing it from ON-OFF DS ganglion cells.

The rabbit G3 ganglion cell (Hoshi and Mills, 2009; Rockhill et al., 2002) also called the vertical orientation cell (Venkataramani and Taylor, 2010) is sometimes referred to as “partly bistratified” (Pu and Amthor, 1990) in that the initial branches in sublamina *b* are sparse and comparatively free of dendritic specializations. While the branching depths are fairly similar to that of the ON bistratified ganglion cell, the two cell types could never be mistaken due to difference in size, branching patterns, distinctive differences in coupled amacrine cells, and other morphological features.

Amthor and colleagues stained a cell (Amthor et al., 1989; Pu and Amthor, 1990) with similar stratification levels, including a diving process (Amthor et al., 1989). Physiologically, the cell was classified as a “uniformity detector”, which has a high maintained discharge which diminishes in response to any change in stimulation. In

numerous recordings from ON bistratified ganglion cells, we never encountered this type of response, leading us to conclude the cells do not correspond.

In agreement with this conclusion, Vaney and colleagues (Sivyer et al., 2010; Sivyer and Vaney, 2010) regularly stained and recorded from a cell they identify as the rabbit uniformity detector. They argue that, while the ON bistratified cell is similar to the uniformity detector in the stratification levels of the dendrites, dendritic branching patterns, and recurrent dendrites, the cells are likely to be different types based upon differences in inhibition in the uniformity detector and the ON bistratified cell (Roska et al., 2006). In addition to these arguments, with which we agree, the primary amacrine cell type tracer-coupled to ON bistratified ganglion cells is distinctly different from the amacrine cell coupled to the uniformity detector, (Sivyer and Vaney, 2010; their Fig. 7) and its soma is located in the ganglion cell layer. Additional differences include the regularity of the dendritic field radius at which recurrent processes dive in ON bistratified ganglion cells (Figs. 1, 4) compared to uniformity detectors and the lack of an tertiary stratification in the middle of the IPL (Fig. 4E; cf. Figs. 3, 4 of Sivyer and Vaney 2010). Finally, the physiology of uniformity detectors is unique and distinctly different from ON bistratified ganglion cells and L-APB abolished only the ON response of uniformity detectors (Sivyer et al., 2010), while it abolished all responding in ON bistratified ganglion cells. Another type of bistratified ganglion cell (Sivyer et al., 2011) also has dendrites that branch in both ON and OFF sublaminae, but whose branches do not ramify at the same levels as the ON bistratified ganglion cell or uniformity detector.

Roska and colleagues (Roska et al., 2006; Roska and Werblin, 2001; 2003) recorded from a population of bistratified ganglion cells that they called Type 9 or ON bistratified. Although they did not note a recurrent pattern in the dendritic field, we nevertheless believe that this type likely corresponds to the diving ON bistratified ganglion cell described here, as the stratification pattern is similar and all light responses were abolished in L-APB, as in our results (Fig. 8B, C; Hoshi et al., 2009). This ganglion cell type had a sustained response and was not suppressed by rapid global motion of natural scene stimuli. While the L-APB experiments indicate that all excitation derives from the ON pathway, Roska and Werblin (2001) found that all inhibition derived from the OFF pathway.

Morphologically, ON bistratified ganglion cells have not been clearly described previously in the rabbit or other retinas. Their morphology presumably produces a unique filtering function for visual stimuli; however the filtering characteristics and overall visual function of this ganglion cell type have not yet been established. The function of the descending dendrites and also the presence of an OFF arbor that does not receive excitatory input from OFF bipolar cells are both unclear. In general, ganglion cells receive cross-laminar inhibitory input from glycinergic amacrine cells that ramify in both sublaminae (Chen et al. 2010). The purpose of sending dendrites high in sublamina *a* could be because the desired inputs are from GABA-releasing amacrine cells, which were not found to participate in crossover inhibition (Chen et al. 2010).

Acknowledgments

This research was supported by NIH grants EY 06515 to SCM, EY 10121 to SLM and Vision Core Grant EY10608, and by an unrestricted award from Research to Prevent Blindness to the Department of Ophthalmology and Visual Science, University of Texas at Houston Health Science Center.

REFERENCE LIST

Amthor FR, Oyster CW, Takahashi ES. Morphology of on-off direction-selective ganglion cells in the rabbit retina. Brain Res. 1984; 298:187–190. [PubMed: 6722555]

Amthor FR, Takahashi ES, Oyster CW. Morphologies of rabbit retinal ganglion cells with complex receptive fields. J Comp Neurol. 1989; 280:97–121. [PubMed: 2918098]

Anadón R, Molist P, Rodriguez-Moldes I, Lopez JM, Quintela I, Cervino MC, Barja P, Gonzalez A. Distribution of choline acetyltransferase immunoreactivity in the brain of an elasmobranch, the lesser spotted dogfish (Scyliorhinus canicula). J Comp Neurol. 2000; 420:139–170. [PubMed: 10753304]

Barlow HB, Hill RM, Levick WR. Retinal ganglion cells responding selectively to direction and speed of image motion in the rabbit. J Physiol. 1964; 173:377–407. [PubMed: 14220259]

Brainard DH. The Psychophysics Toolbox. Spatial Vision. 1997; 10:443–446. [PubMed: 9176954]

Caldwell JH, Daw NW, Wyatt HJ. Effects of picrotoxin and strychnine on rabbit retinal ganglion cells: lateral interactions for cells with more complex receptive fields. J Physiol. 1978; 276:277–298. [PubMed: 650450]

Chen X, Hsueh HA, Greenberg K, Werblin FS. Three forms of spatial temporal feedforward inhibition are common to different ganglion cell types in rabbit retina. J Neurophysiol. 2010; 103:2618–2632. [PubMed: 20220071]

Famiglietti EV. 'Starburst' amacrine cells and cholinergic neurons: mirror-symmetric on and off amacrine cells of rabbit retina. Brain Res. 1983; 261:138–144. [PubMed: 6301622]

Famiglietti EV. Bistratified ganglion cells of rabbit retina: neural architecture for contrast-independent visual responses. Vis Neurosci. 2009; 26:195–213. [PubMed: 19272195]

Farrow K, Masland RH. Physiological clustering of visual channels in the mouse retina. J Neurophysiol. 2011; 105:1516–1530. [PubMed: 21273316]

Hattar S, Liao HW, Takao M, Berson DM, Yau KW. Melanopsin-containing retinal ganglion cells: architecture, projections, and intrinsic photosensitivity. Science. 2002; 295:1065–1070. [PubMed: 11834834]

Hildebrand JD, Soriano P. Overlapping and unique roles for C-terminal binding protein 1 (CtBP1) and CtBP2 during mouse development. Mol Cell Biol. 2002; 22:5296–5307. [PubMed: 12101226]

Hoshi H, Liu WL, Massey SC, Mills SL. ON inputs to the OFF layer: bipolar cells that break the stratification rules of the retina. J Neurosci. 2009; 29:8875–8883. [PubMed: 19605625]

Hoshi H, Mills SL. Components and properties of the G3 ganglion cell circuit in the rabbit retina. J Comp Neurol. 2009; 513:69–82. [PubMed: 19107780]

Hoshi H, Tian LM, Massey SC, Mills SL. Two distinct types of ON directionally selective ganglion cells in the rabbit retina. J Comp Neurol. 2011; 519:2509–2521. [PubMed: 21618235]

Kanjhan R, Vaney DI. Semi-loose seal Neurobiotin electroporation for combined structural and functional analysis of neurons. Pflugers Arch. 2008; 457:561–568. [PubMed: 18600343]

Lamb TD, Simon EJ. The relation between intercellular coupling and electrical noise in turtle photoreceptors. J Physiol. 1976; 263:257–286. [PubMed: 1018249]

Lewis DA, Melchitzky DS, Haycock JW. Four isoforms of tyrosine hydroxylase are expressed in human brain. Neurosci. 1993; 54:477–492.

Liu W-L, Hoshi H, Pan F, Kim I-B, Mills SL, Massey SC. Melanopsin ganglion cells in the rabbit retina. ARVO Meeting Abstracts. 2008; 49:1411.

Marc RE, Jones BW. Molecular phenotyping of retinal ganglion cells. J Neurosci. 2002; 22:413–427. [PubMed: 11784786]

Massey SC, Mills SL. A calbindin-immunoreactive cone bipolar cell type in the rabbit retina. J Comp Neurol. 1996; 366:15–33. [PubMed: 8866843]

Oyster CW. The analysis of image motion by the rabbit retina. J Physiol. 1968; 199:613–635. [PubMed: 5710424]

Oyster CW, Barlow HB. Direction-selective units in rabbit retina: distribution of preferred directions. Science. 1967; 155:841–842. [PubMed: 6019094]

Pelli DG. The VideoToolbox software for visual psychophysics: Transforming numbers into movies. Spatial Vision. 1997; 10:437–442. [PubMed: 9176953]

Pow DV, Wright LL, Vaney DI. The immunocytochemical detection of amino-acid neurotransmitters in paraformaldehyde-fixed tissues. J Neurosci Meth. 1995; 56:115–123.

Pu ML, Amthor FR. Dendritic morphologies of retinal ganglion cells projecting to the lateral geniculate nucleus in the rabbit. J Comp Neurol. 1990; 302:675–693. [PubMed: 1702124]

Rockhill RL, Daly FJ, MacNeil MA, Brown SP, Masland RH. The diversity of ganglion cells in a mammalian retina. J Neurosci. 2002; 22:3831–3843. [PubMed: 11978858]

Roska B, Molnar A, Werblin FS. Parallel processing in retinal ganglion cells: how integration of space-time patterns of excitation and inhibition form the spiking output. J Neurophysiol. 2006; 95:3810–3822. [PubMed: 16510780]

Roska B, Werblin F. Vertical interactions across ten parallel, stacked representations in the mammalian retina. Nature. 2001; 410:583–587. [PubMed: 11279496]

Roska B, Werblin F. Rapid global shifts in natural scenes block spiking in specific ganglion cell types. Nat Neurosci. 2003; 6:600–608. [PubMed: 12740583]

Schmitz F, Konigstorfer A, Sudhof TC. RIBEYE, a component of synaptic ribbons: a protein's journey through evolution provides insight into synaptic ribbon function. Neuron. 2000; 28:857–872. [PubMed: 11163272]

Sivyer B, Taylor WR, Vaney DI. Uniformity detector retinal ganglion cells fire complex spikes and receive only light-evoked inhibition. Proc Natl Acad Sci U S A. 2010; 107:5628–5633. [PubMed: 20212117]

Sivyer B, Vaney DI. Dendritic morphology and tracer-coupling pattern of physiologically identified transient uniformity detector ganglion cells in rabbit retina. Vis Neurosci. 2010; 27:159–170. [PubMed: 20854715]

Sivyer B, Venkataramani S, Taylor WR, Vaney DI. A novel type of complex ganglion cell in rabbit retina. J Comp Neurol. 2011; 519:3128–3138. [PubMed: 21800303]

Taylor WR, Vaney DI. Diverse synaptic mechanisms generate direction selectivity in the rabbit retina. J Neurosci. 2002; 22:7712–7720. [PubMed: 12196594]

tom Dieck S, Altrock WD, Kessels MM, Qualmann B, Regus H, Brauner D, Fejtova A, Bracko O, Gundelfinger ED, Brandstatter JH. Molecular dissection of the photoreceptor ribbon synapse: physical interaction of Bassoon and RIBEYE is essential for the assembly of the ribbon complex. J Cell Biol. 2005; 168:825–836. [PubMed: 15728193]

Vaney DI. Territorial organization of direction-selective ganglion cells in rabbit retina. J Neurosci. 1994; 14:6301–6316. [PubMed: 7965037]

van Wyck M, Taylor WR, Vaney DI. Local edge detectors: a substrate for fine spatial vision at low temporal frequencies in rabbit retina. J Neurosci. 2006; 26:13250–13263. [PubMed: 17182775]

Venkataramani S, Taylor WR. Orientation selectivity in rabbit retinal ganglion cells is mediated by presynaptic inhibition. J Neurosci. 2010; 30:15664–15676. [PubMed: 21084622]

Viney TJ, Balint K, Hillier D, Siegert S, Boldogkoi Z, Enquist LW, Meister M, Cepko CL, Roska B. Local retinal circuits of melanopsin-containing ganglion cells identified by transsynaptic viral tracing. Curr Biol. 2007; 17:981–988. [PubMed: 17524644]

Wässle H. Parallel processing in the mammalian retina. Nat Rev Neurosci. 2004; 5:747–757. [PubMed: 15378035]

Wyatt HJ, Daw NW. Directionally sensitive ganglion cells in the rabbit retina: specificity for stimulus direction, size, and speed. J Neurophysiol. 1975; 38:613–626. [PubMed: 1127460]

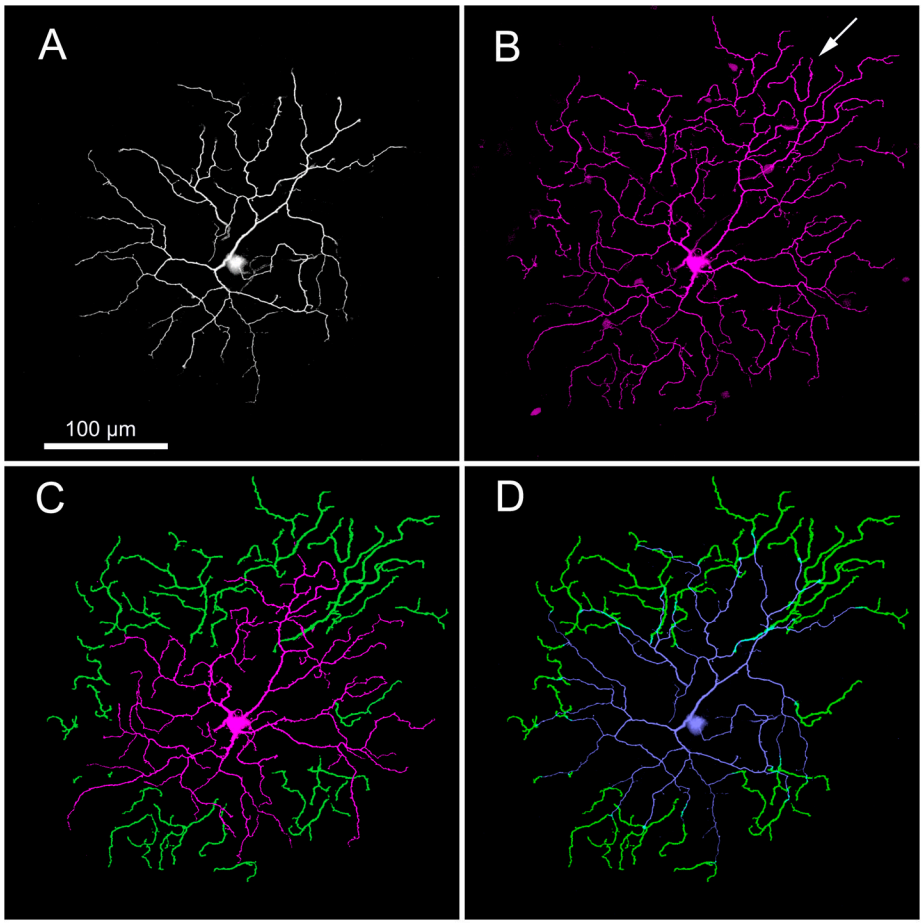

Figure 1.

Neurobiotin-staining of one type of rabbit ganglion cell reveals a bistratified dendritic tree with recurrent dendrites. (A) Focus on sublamina *a* shows that one set of dendrites ascends to and arborizes in the OFF sublamina. (B) Focus on sublamina *b* shows a second set of dendrites that arborize in the ON sublamina. However, a number of terminal dendrites can be seen in sublamina *b* that are not visibly connected to the soma in these layers (e.g., arrow). (C) Juxtaposition of the disconnected dendrites in sublamina *b* (green) highlights that they are not continuous with the remaining ON dendrites (red). (D) Juxtaposition of the disconnected dendrites in sublamina *b* (green) with the OFF dendritic arbor (gray) reveals that these dendrites originate from rapidly descending processes that originally arborized in sublamina *a*. These micrographs are stacks of 16 × 1 μm optical sections. This cell was 5.2 mm ventral to the visual streak. Increasing the gain of the green dendrites for emphasis produced a slight thickening of the dendrites compared to the other dendrites.

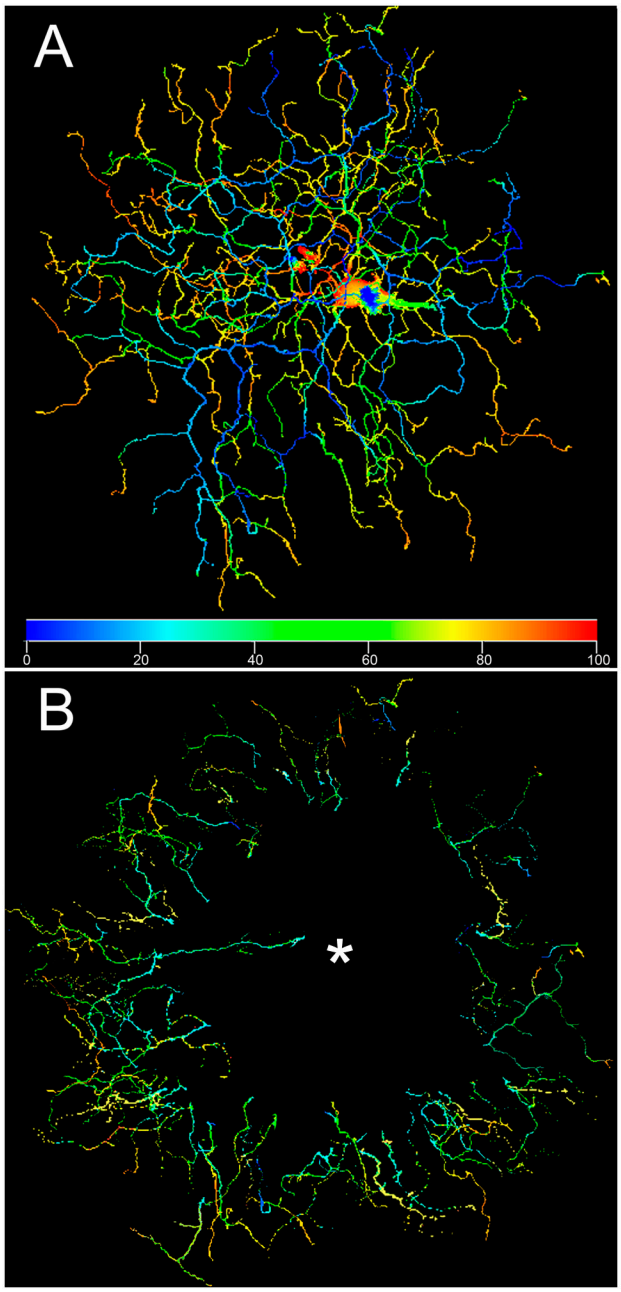

Figure 2.

(A) Another ganglion cell of this type is shown with the color of its branches coded according to depth in the INL, where the proximal dendrites are red and the distal dendrites blue. At several locations near the periphery of the ganglion cell dendritic field, dendrites in sublamina *a* (blue) can be seen to rapidly descend to sublamina *b* (red/orange). This cell was about 6 mm ventral to the visual streak. (B) A montage of the descending processes from 10 examples of this ganglion cell type show that the diving portion of the dendritic arbor almost invariably occurs at about 70% of the dendritic field radius. Each ganglion cell was scanned with 0.3 μm optical sections from the location of the most proximal branch in sublamina *b* to the most distal branch in sublamina *a* in order to standardize the color coding as much as possible. The asterisk marks the common position of the somas.

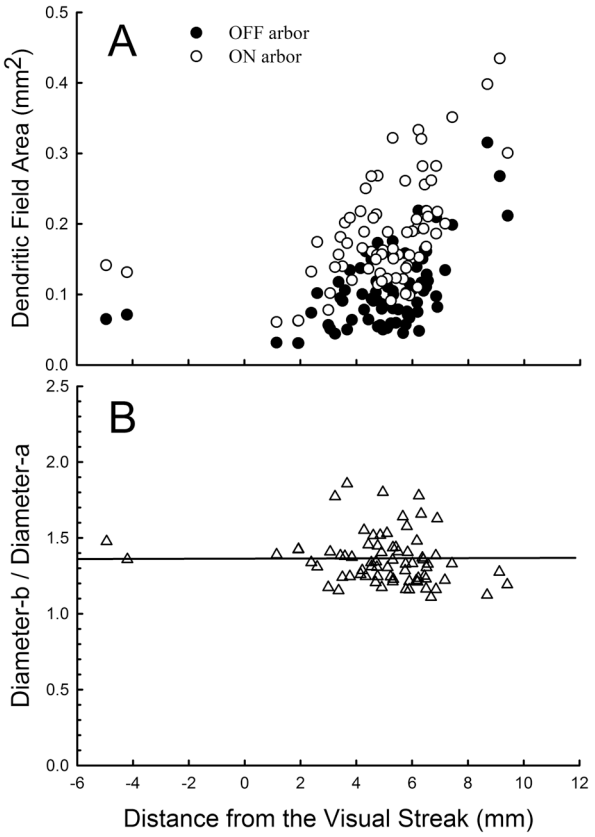

Figure 3.

(A) The area of the ON and OFF arbors of 74 ON bistratified ganglion cells is shown as a function of distance from the visual streak. (B) The ratio of the ON to OFF arbor does not vary systematically with eccentricity, but remains constant at about 1.4.

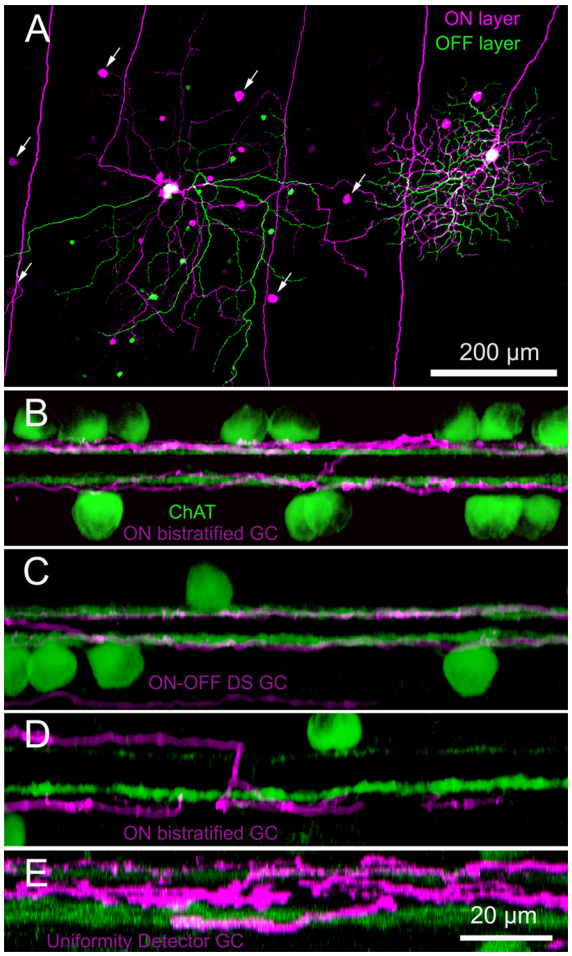

Figure 4.

A comparison of ON bistratified and ON-OFF DS ganglion cells. (A) Staining of adjacent bistratified and ON-OFF DS ganglion cells illustrates the relative size differences as well as differences in the branching patterns. This micrograph is color-coded for depth (green=distal; magenta=proximal). Arrows mark Neurobiotin-coupled ON bistratified ganglion cells. While ON-OFF DS ganglion cells (C; magenta) are well known to stratify within the ON and OFF bands formed by starburst amacrine cells (green), ON bistratified ganglion cell processes (B, D; magenta) stratify just above and below these bands. (D) A diving process from a ON bistratified ganglion cell illustrates the characteristic abrupt descent from sublamina *a* to sublamina *b* that occurs just beyond the spatial extent of the dendritic arbor that is wholly contained in sublamina *b*. Two uniformity detectors each contain processes at intermediate depths in the IPL, with branches that shift level at many different distances from the soma. The micrograph in (A) is a stack of 32 × 1 µm optical sections. (B–D) z-rotations of stacks of 35–48 × 0.3 µm optical sections. (E,F) z-rotations of stacks of 34 and 37 µm optical sections. Cells labeled cyan in (F) are ganglion and amacrine cells stained with DAPI. Scale bar in (B) also applies to (C,D); scale bar in (F) also applies to (E). Distances (mm) ventral to the visual streak: (A–F) 5, 7, 6.5, 6.2, 5, 3.2.

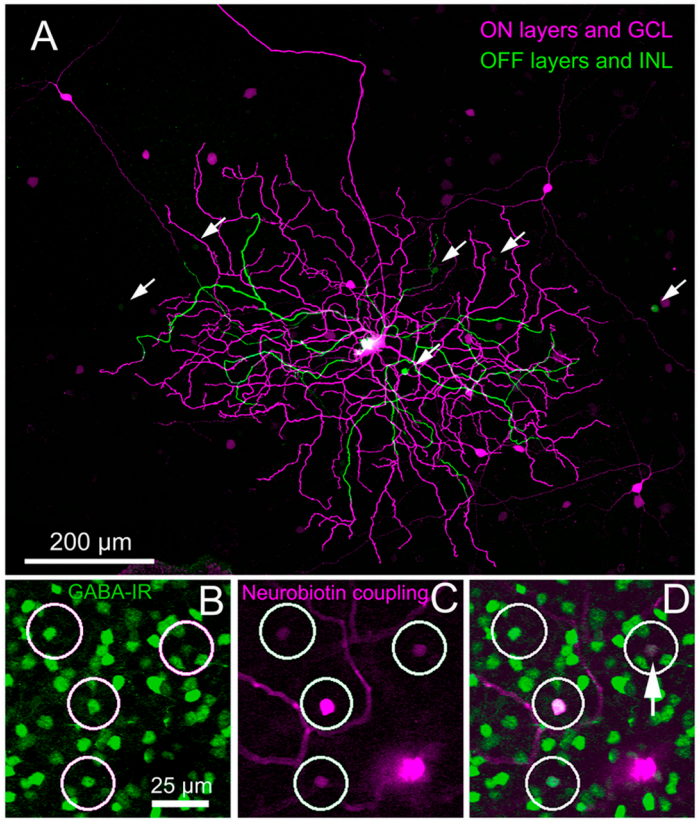

Figure 5.

(A) A Neurobiotin-injected ON bistratified ganglion cell is color-coded for depth (magenta is proximal; green is distal). Several amacrine cells with large somas (magenta) can be seen to have their somas displaced to the ganglion cell layer. Somas of a smaller amacrine cell type (green) are conventionally placed in the inner nuclear layer. (B–D) Amacrine cells seen after Neurobiotin-injection into another ON bistratified ganglion cell were colabeled with an antibody to GABA. (B) GABA-immunoreactive amacrine cells within a small region of the dendritic field. The larger magenta soma belongs to the injected ganglion cell. (C) Four coupled amacrine cells are shown. (D) Colocalization of Neurobiotin (magenta) and anti-GABA (green) signals. Somas of 3 of the amacrine cells were displaced to the GCL; the other was in the amacrine cell layer (arrow). Micrographs are stacks of (A) 25 × 1 μm and (B–D) 79 × 0.3 μm optical sections.

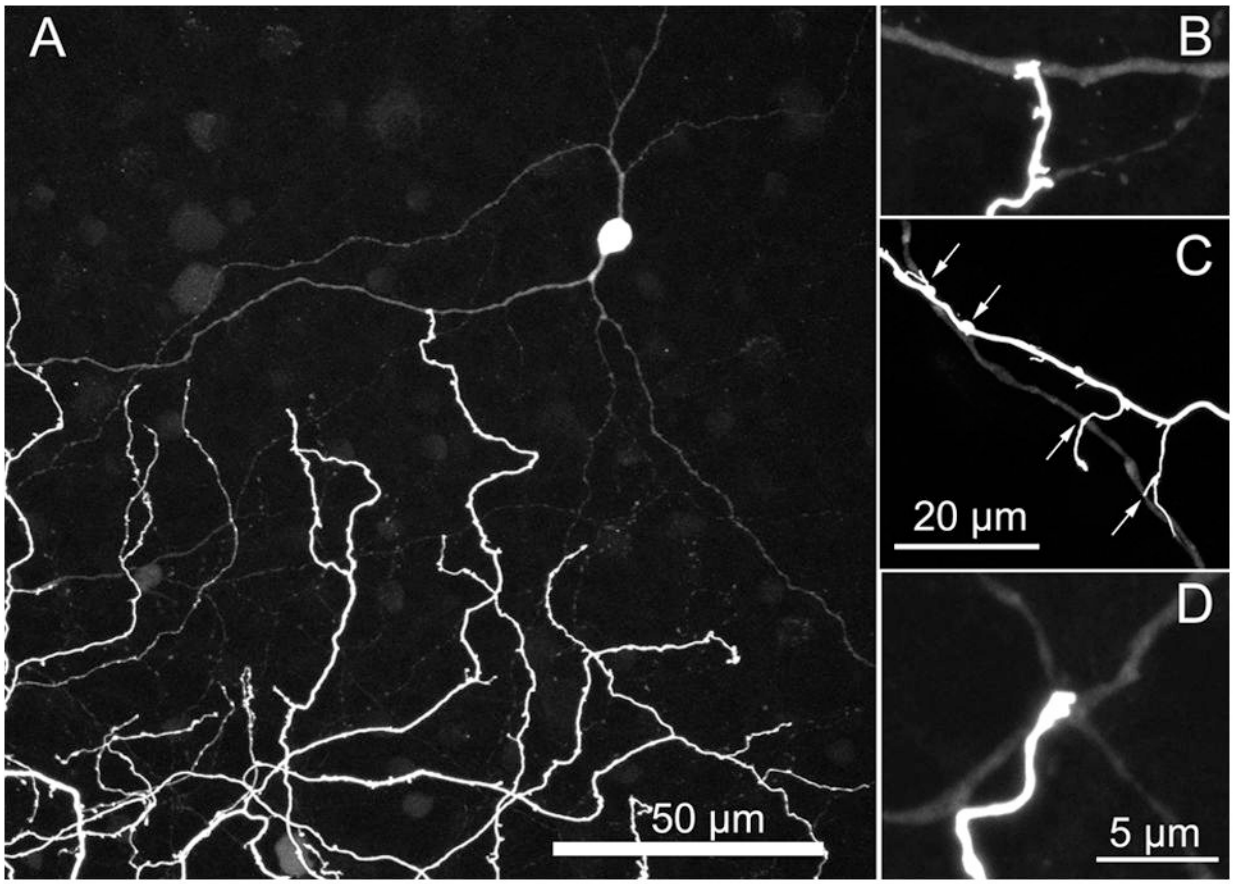

Figure 6.
(A) The large displaced amacrine cells have a characteristic morphology with two dendrites emerging from opposite ends of soma and running 10–25 µm before branching. (B–D) Terminal varicosities from dendrites of ON bistratified ganglion cells frequently terminate on a dendrite of one of the coupled amacrine cells. The amacrine cell in B is a magnified view of the amacrine cell in A. Micrographs are stacks of (A) 22 × 1 µm (B,D) 1 × 0.3 µm (c) 3 × 0.3 µm optical sections.

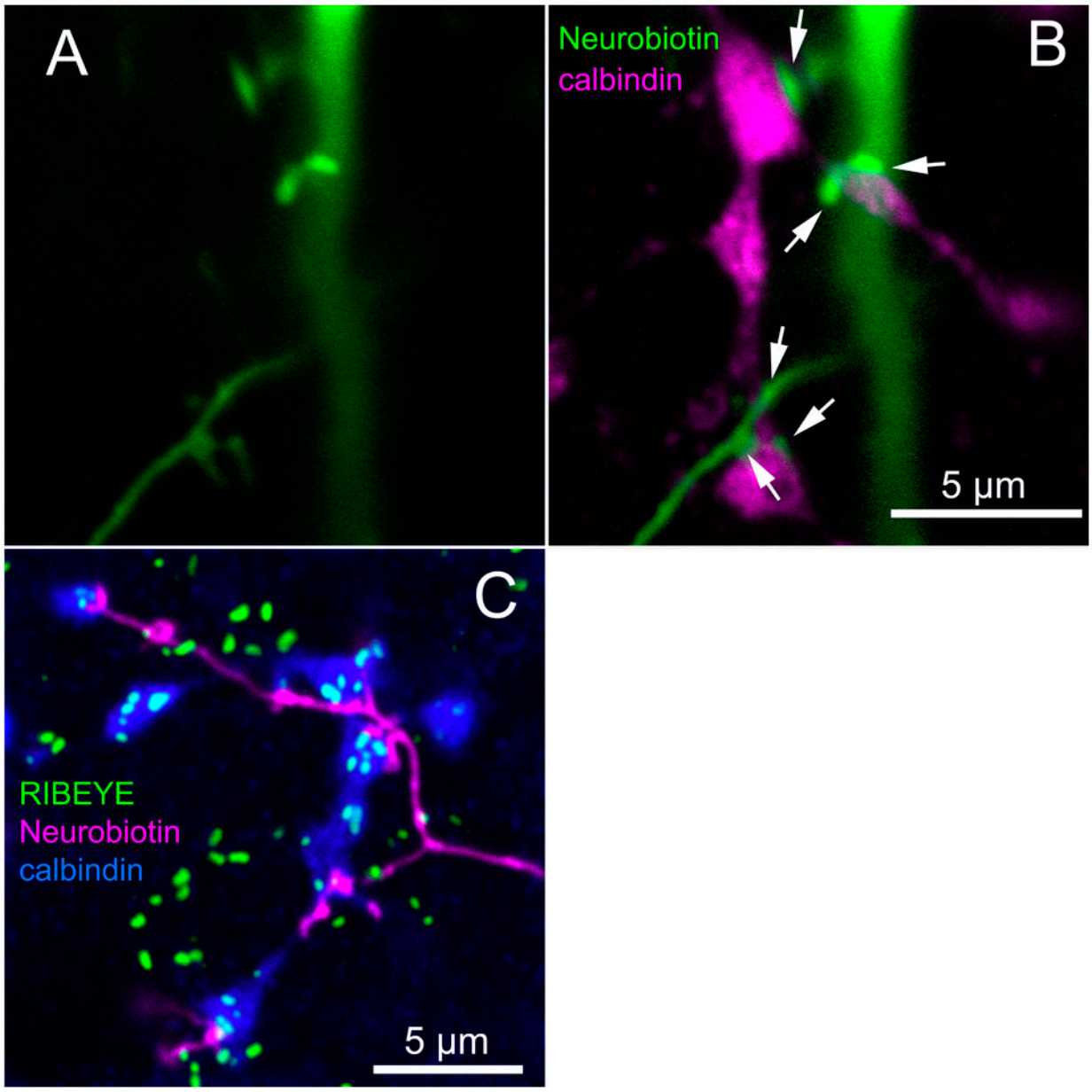

Figure 7.

(A, B) The axon terminals of calbindin-positive ON cone bipolar cells (green) routinely contact dendritic specializations from the ON arbor of ON bistratified ganglion cells (magenta). (C) RIBEYE (green), a marker for synaptic ribbons, is contained in these axon terminals (blue) and apposes the contacts from the ON bistratified ganglion cells (magenta)

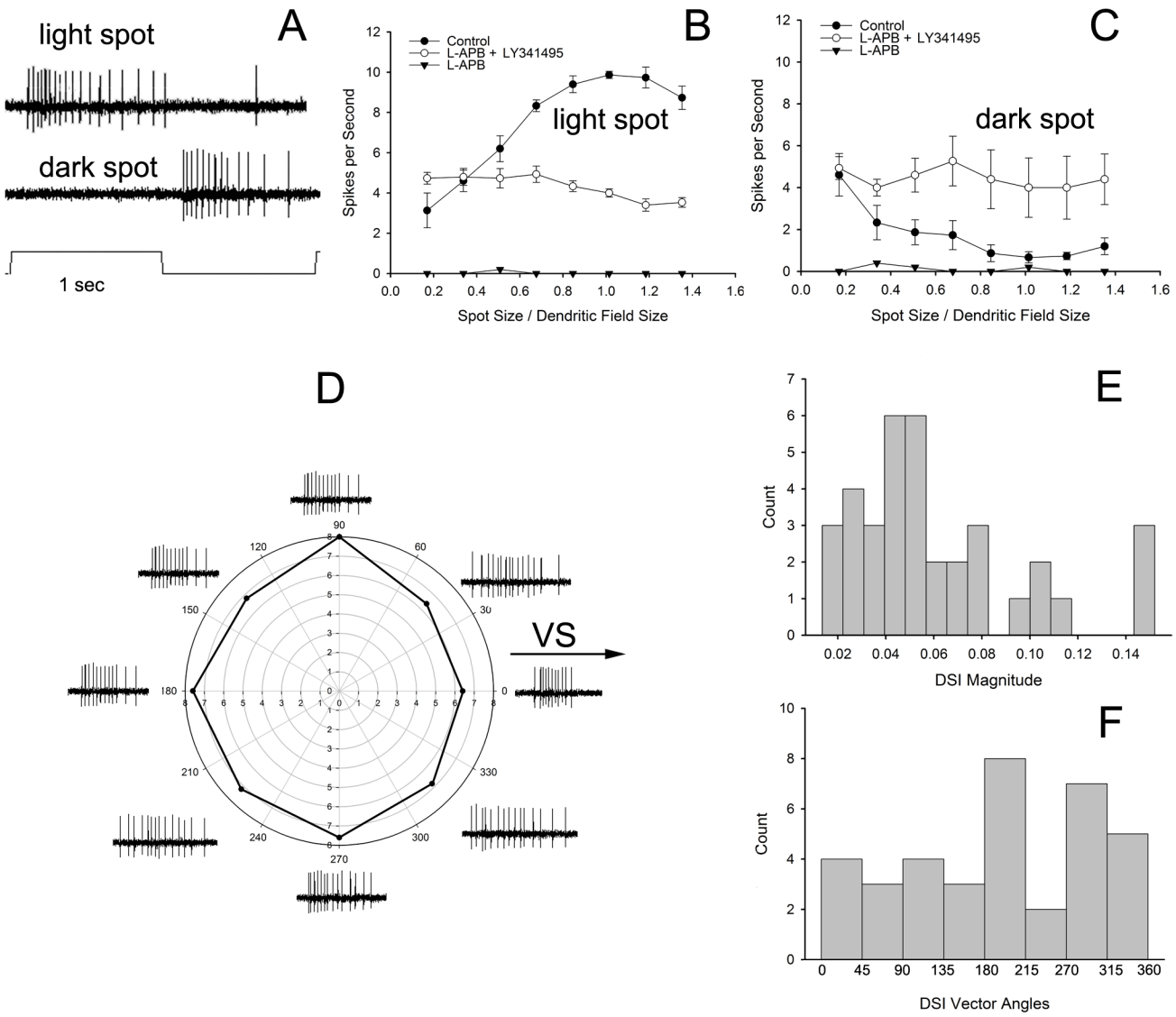

Figure 8.

(A) A light spot centered on a ON bistratified ganglion cell and covering the receptive field produced spiking only to the onset of the stimulus, while a dark spot of the same size caused spiking only at stimulus offset. (B) Light spots of increasing diameter produced a receptive field with a maximal response near the dendritic field size. The mGluR6 agonist L-APB (25 μM) abolished all light-driven activity; combining L-APB with a mGluR6 antagonist LY341495 (50 μM) restored spiking activity with no light-driven component. (C) The onset of dark spots of increasing diameter produced little stimulus-driven activity. L-APB abolished almost all spiking. LY341495 restored spiking, but did not unmask any stimulus-driven activity hidden by mGluR6-mediated ON bipolar cell activity. (D) Representative responses of a ON bistratified ganglion cell to light bars moving in 8 different directions. The arrow shows the direction with respect to of the visual streak. A polar plot of these responses reveals little directional preference; the vector magnitude = 0.031 with an angle of 185°. The diameters of the concentric circles represent spikes/sec. Movement toward the visual streak is 0°. (E) The magnitude of the directional responses averaged only .061 (s.d. = 0.037), while the vector angles (F) did not show clearly defined clusters in a few cardinal

directions. Responses in (B) and (C) are the averages of 4 cells from 6–8 mm inferior to the visual streak and with dendritic fields from 605–665 μm in diameter.

Table 1

Antibodies Used and Their Immunogens, Suppliers, and Dilutions.

antigen	immunogen	manufacturer, species, type, catalog number	Dilution used
Choline acetyltransferase	human placental enzyme	Millipore, Inc. (Billerica, MA) goat polyclonal #AB144P	1:100
RIBEYE	CtBP2 C-term. a.a. 361–445	BD Biosciences (San Jose, CA) mouse monoclonal, #612044	1:500
Calbindin D-28 (CB)	recombinant rat CB	Swant (Switzerland) rabbit polyclonal, #CB38	1:5,000
Tyrosine hydroxylase (TOH)	rat TOH a.a. 40–152	Sigma, Inc. (St. Louis, MO) mouse monoclonal #T2928	1:10,000
GABA	formaldehyde conjugate - porcine thyroglobulin	Immunosolution Pty Ltd (Jesmond, NSW, AU) rabbit polyclonal #IG1004	1:1,000